Modelling of confined vortex rings with a core of elliptical cross- section

Felix Kaplanski[1]

[1]Tallinn University of Technology, Estonia

Research Workshop, Brighton, Tuesday, 14th July, 2015

Outline

1. Models of vortex ring in unbounded domains
   - An unconfined vortex ring with a core of circular cross- section
   - An unconfined vortex ring with a core of elliptical cross- section
2. Models of vortex ring in confined domains
   - A model for a viscous vortex ring in a tube: Governing equations
   - Vortex ring with a core of circular cross- section in a tube
   - Vortex ring with a core of elliptic cross- section in a tube
3. Fit of the DNS vortex ring with the vortex ring models
   - Comparison procedure
   - Re=1700, t=8
   - Re=3400, t=15
4. Formation number
5. Conclusions

Scheme of a vortex ring

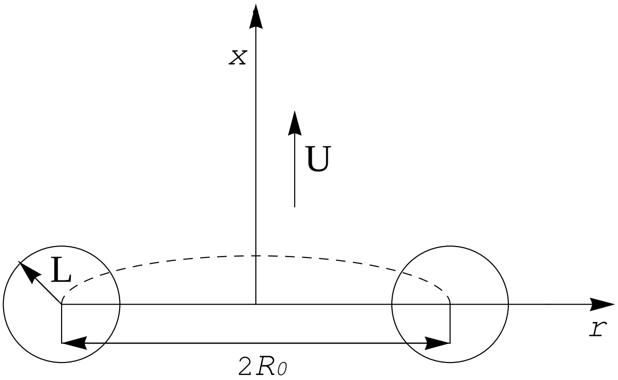

Model based on the linear first-order solution to the Navier−Stokes equation for the axisymmetric geometry and arbitrary times,(Kaplanski&Rudi, PF 2005, hereinafter Model I):

$$\omega_{VR} = \frac{\Gamma_0 \theta^3}{\sqrt{2\pi} R_0^2} \exp\left(-\frac{\sigma^2 + \eta^2 + \theta^2}{2}\right) \mathrm{I}_1\left(\sigma\theta\right),$$

$$\Psi_{VR} = \frac{\Gamma_0 R_0 \sigma}{4} \int_0^\infty F(\mu, \eta) \mathrm{J}_1(\theta\mu) \mathrm{J}_1(\sigma\mu) d\mu,$$

where

$$F(\mu, \eta) = \exp(\eta\mu)\mathrm{erfc}\left(\frac{\mu+\eta}{\sqrt{2}}\right) + \exp(-\eta\mu)\mathrm{erfc}\left(\frac{\mu-\eta}{\sqrt{2}}\right),$$

$$\eta = \frac{(x - X_c)}{L}, \quad \sigma = \frac{r}{L}, \quad \theta = \frac{R_0}{L},$$

$$\Gamma_0 = \frac{M}{\pi R_0^2}, \quad M = \pi \int_0^\infty \int_{-\infty}^\infty r^2 \omega dx dr,$$

$$\Gamma = \Gamma_0 \left\{ 1 - \exp\left(-\frac{\theta^2}{2}\right) \right\}, \quad \Gamma_0 = \frac{M}{\pi {R_0}^2},$$

$$E = \frac{\Gamma_0^2 R_0 \theta}{2} [\frac{1}{12} \sqrt{\pi} \theta^2 {}_2\mathrm{F}_2 \left(\{\frac{3}{2}, \frac{3}{2}\}, \{\frac{5}{2}, 3\}, -\theta^2 \right)],$$

$$U = \frac{\Gamma_0 \theta \sqrt{\pi}}{4\pi R_0} [3 \exp(-\frac{\theta^2}{2}) \mathrm{I}_1 \left(\frac{\theta^2}{2} \right)$$

$$+ \frac{\theta^2}{12} {}_2\mathrm{F}_2 \left(\{\frac{3}{2}, \frac{3}{2}\}, \{\frac{5}{2}, 3\}, -\theta^2 \right) - \frac{3\theta^2}{5} {}_2\mathrm{F}_2 \left(\{\frac{3}{2}, \frac{5}{2}\}, \{2, \frac{7}{2}\}, -\theta^2 \right) \Big],$$

Distribution of the vorticity in the Model I

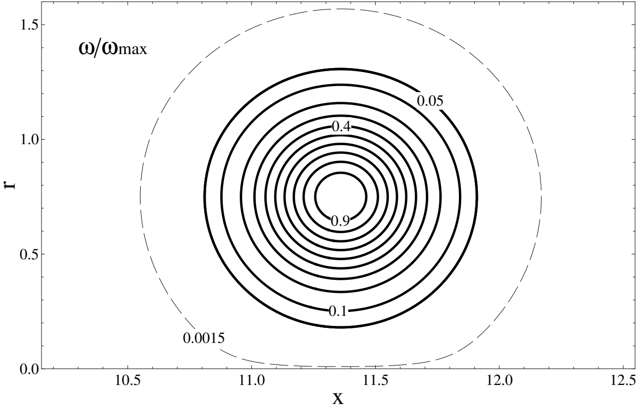

Figure: Isocontours of the normalized vorticity $\omega/\omega_{\text{max}}$ for the values $\theta = 3.56$, $R_0 = 0.783$ and $X_0 = 11.36$, that give best fit of the theoretical vortex to the simulated vortex (Danaila&Helio PF 2008). The dashed line represents contour for $\omega/\omega_{\text{max}} = 0.0015$.

Concluding Remarks

- All characteristics of vortex rings, including kinetic energy and translational velocity , were given by the closed-form expressions and at short and long times their asymptotic were identical to the well-known Saffman and Rott&Cantwell formulae, respectively.
- The Model I was originally developed for $L = \sqrt{2\nu t}$, i.e. a laminar vortex ring. Later it was shown that it remain valid in a more general case, when L is approximated as at^b, where a and b are constants $1/4 \leq b \leq 1/2$ (Kaplanski et al.2009). This generalised vortex ring model was successfully applied to the analysis of vortex rings observed in petrol internal combustion engines (Begg et al. 2009; Kaplanski et al. 2010).
- The Model I, which was developed on the basis of the circular ring core, does not take into account Reynolds-number effect and predicts the translation velocity and normalized energy rather roughly with a relative error of 10%.

An unconfined vortex ring with a core of elliptical cross- section (Kaplanski et al., PF 20012, hereinafter Model II):

$$\omega_{VRE} = \frac{\Gamma_0 \theta_e^3}{R_0^2 \beta \sqrt{2\pi}} \exp\left(-\frac{(\sigma^2 + (\eta/\beta)^2 + \theta_e^2)}{2}\right) \mathrm{I}_1(\sigma\theta_e),$$

$$\Psi_{VRE} = \frac{\Gamma_0 R_0 \theta_e \sigma}{4} \int_0^\infty \exp((\beta^2 - 1)\mu^2/2)[\exp(-\eta\mu)\mathrm{erfc}(\frac{\mu\beta - \eta/\beta}{\sqrt{2}})$$

$$+ \exp(\eta\mu)\mathrm{erfc}(\frac{\mu\beta + \eta/\beta}{\sqrt{2}})]\mathrm{J}_1(\mu\theta_e)\,\mathrm{J}_1(\sigma\mu)\,d\mu,$$

where $\theta_e = (R_0/L_e)$, with L_e the new viscous length scale:

$$\theta_e = \frac{R_0}{L_e} = \lambda\theta \Longrightarrow L_e = \frac{L}{\lambda},$$

and parameters $\beta > 0$ and $\lambda > 0$ measure elongation and compression along axes x and r, respectively.

Characteristics of a vortex ring with a core of elliptical cross-section

$$\Gamma_e = \Gamma_0 \left(1 - \exp\left(-\frac{\theta_e^2}{2} \right) \right),$$

$$E_e = \frac{\Gamma_0^2 R_0 \pi \theta_e}{2} \int_0^\infty \exp((\beta^2 - 1)\mu^2)\, \mathrm{erfc}(\beta\mu)\, \mathrm{J}_1^2(\theta_e \mu)\, d\mu,$$

$$U_e = \frac{\Gamma_0 \theta_e}{4\pi R_0} \int_0^\infty \exp(-\mu^2)[6\sqrt{\pi}\beta\mu$$

$$+\pi \exp(\beta^2\mu^2)(1 - 6\beta^2\mu^2)\mathrm{erfc}(\beta\mu)]\mathrm{J}_1^2(\theta_e\mu)d\mu,$$

Vorticity and streamfunction distributions in the Model II

a)

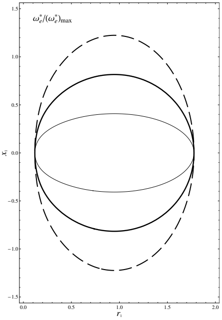

b)

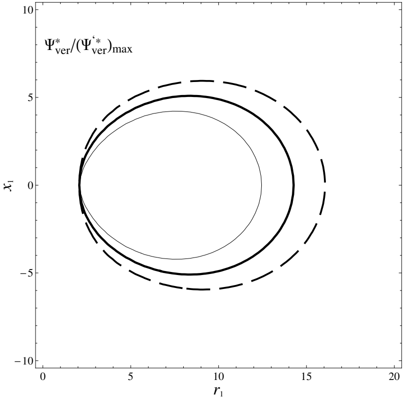

Figure: Model of a vortex ring with elliptical core for $\lambda = 1$ and $\theta = 3$. a) Normalised vorticity contours $\omega^*_{VRE}/(\omega^*_{VRE})_{max} = 0.05$. b) Isocontours of the stream function $\Psi^*_{VRE}/(\Psi^*_{VRE})_{max} = 0.3$. $\beta = 1.5$ (dashed line), $\beta = 1$ (thick solid line) and for $\beta = 0.5$ (thin solid line).

Ellipticity dependence in the Model II

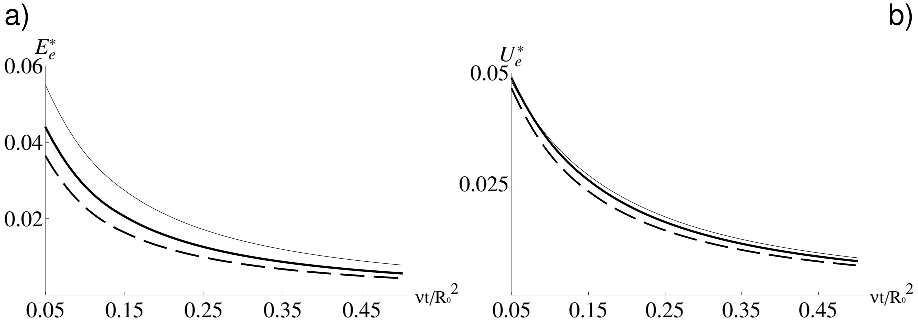

Figure: Model of a vortex ring with elliptical core for $\lambda = 1$ and $\theta = 3$. a) Time evolution of the kinetic energy E_e^*. b) Time evolution of the translation velocity U_e^*. $\beta = 1.5$ (dashed line), $\beta = 1$ (thick solid line) and for $\beta = 0.5$ (thin solid line).

Conditions related to time limits:

$$\beta = 1 + \epsilon_0\theta_0/\theta, \lambda = 1 + \lambda_0\theta_0/\theta \quad (\theta > \theta_0), (\textit{small time})$$

$$\beta = 1 + \epsilon_0\theta/\theta_0, \lambda = 1 + \lambda_0\theta/\theta_0 \quad (\theta \leq \theta_0), (\textit{large time})$$

where $0 \leq \epsilon_0 < 1$ and $0 \leq \lambda_0 < 1$.

Finding amendments $\epsilon_0 = 0.4$ and $\lambda_0 = 0.16$

$$E_{\mathrm{d}} = E/(M^{1/2}\Gamma^{3/2}) = 0.276, \tag{1}$$

$$\Gamma_{\mathrm{d}} = \Gamma/(M^{1/3}U^{2/3}) = 2.128. \tag{2}$$

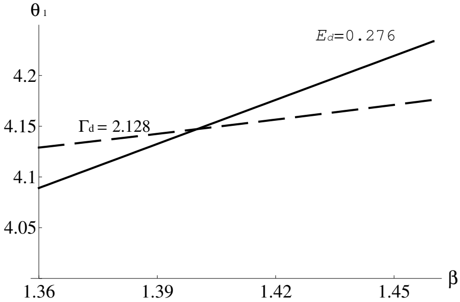

Figure: Intersect of the curves described by Eq.(1) (solid curve) and Eq.(2) (dashed curve).

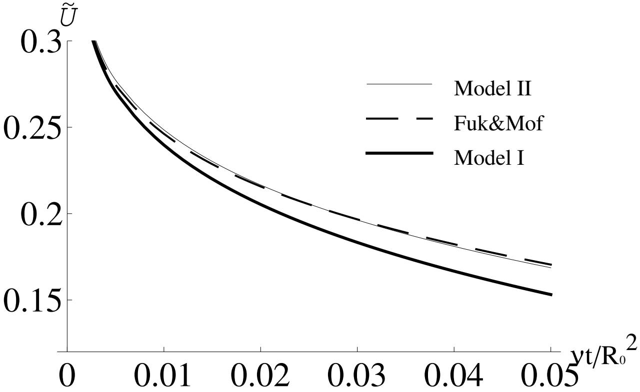

Figure: The temporal evolution of the translation velocity at small times. The dashed line is the large-Reynolds- number asymptotic by Fukumoto&Moffatt(Physica D, 2008) and the thin solid line is the present result with correction ($\beta = 1 + 0.4\theta_0/\theta; \lambda = 1 + 0.16\theta_0/\theta, \theta_0 = 3.56$). The thick solid line corresponds to Model I.

The translation velocity at large times predicted by the Model II

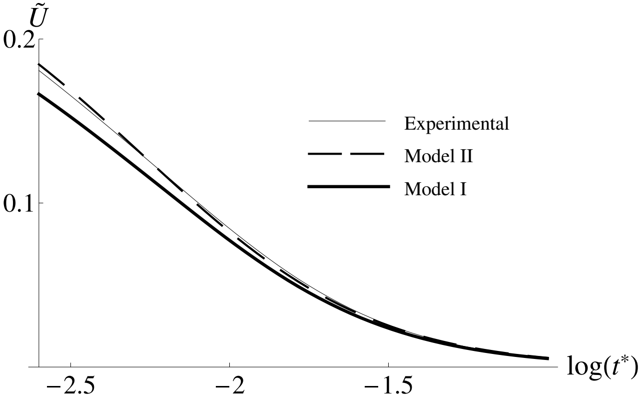

Figure: The temporal evolution of the translation velocity at the postformation phase. The dashed line draw predicted by the formula (Saffman,Stud. Appl. Math. 1970) (corresponds to the experimental data by Wengand&Gharib, Exp. in Fluids,1997) with $k = 14.4$ and $k^{'} = 7.8$, and the thin solid line is the present result with correction ($\beta = 1 + 0.4\theta/\theta_0, \lambda = 1 + 0.16\theta/\theta_0, \theta_0 = 3.56$). The thick solid line corresponds to Model I.

New assumption for the time-dependency, which we will use further:

$$\beta = 1 + \epsilon_0, \lambda = 1 + \lambda_0\theta/\theta_0 \quad (\theta \leq \theta_0), (\textit{large time})$$

Improved Rott&Cantwell (1988) asymptotic velocity for the large t :

$$U_{ef} = \frac{\Gamma_0}{R_0}\frac{\theta^3}{4\sqrt{\pi}}\left(\frac{7}{30} - \frac{\epsilon_0}{14}\right) = (0.0037038 - 0.0011338\epsilon_0)\frac{I}{\rho(\nu t)^{3/2}}$$

$$= U_{ef}(\epsilon_0 = 0.4) = 0.00325027\frac{I}{\rho(\nu t)^{3/2}}, \Gamma_0 = \frac{M}{\pi R_0^2}, M = \frac{I}{\rho}.$$

This asymptotic decay is in agreement with experimental data by Weigand&Gharib, (Exp. in Fluids,1997).

Concluding Remarks

- All characteristics of the vortex rings, including kinetic energy and translational velocity , are obtained in the integral forms and are more complex then an appropriate results for the Model I.

- The Model II takes into account Reynolds-number effect and predicts the translation velocity and normalized energy with relatively good accuracy. The obtained corrections ($\beta = 1.4, \lambda = 1.2$) look universal and are suitable for relatively high Reynolds numbers.

Viscous vortex ring in a tube

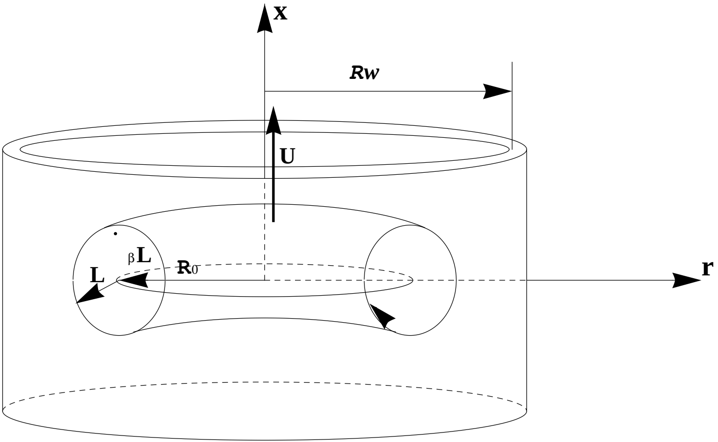

Figure: Schematic of a vortex ring with the elliptical core's cross section in a tube.

A model for a viscous vortex ring in a tube: Governing equations (Danaila et al., JFM 2015), hereinafter Model III

$$\frac{\partial \omega}{\partial t} + \frac{\partial}{\partial r}\left(-\frac{1}{r}\frac{\partial \Psi}{\partial x}\omega\right) + \frac{\partial}{\partial x}\left(\frac{1}{r}\frac{\partial \Psi}{\partial r}\omega\right) = \nu\left(\frac{\partial^2 \omega}{\partial r^2} + \frac{\partial^2 \omega}{\partial x^2} + \frac{1}{r}\frac{\partial \omega}{\partial r} - \frac{\omega}{r^2}\right),$$

$$\frac{\partial^2 \Psi}{\partial r^2} + \frac{\partial^2 \Psi}{\partial x^2} - \frac{1}{r}\frac{\partial \Psi}{\partial r} = -r\omega,$$

where x, r are the axes of a cylindrical coordinate system and t is time. We consider the following boundary conditions:
symmetry at the axis:

$$\omega\left(0, x\right) = \Psi\left(0, x\right) = 0, \quad \text{for} \quad r = 0,$$

and no flow through the tube wall:

$$\omega \to 0, \qquad \frac{1}{r}\frac{\partial \Psi}{\partial x} = 0, \quad \text{for} \quad r = R_w.$$

Brasseur modelled a confined vortex ring assuming that in the region $r > R_0$ the streamfunction Ψ_C is equal to the sum $\Psi_C = \Psi + \Psi_0$, where Ψ is the streamfunction of a circular vortex filament in an unbounded flow:

$$\Psi = \frac{\Gamma_0 R_0 r}{2} \int_0^\infty \exp\left(-x\mu\right) \mathrm{J}_1(R_0\mu) \mathrm{J}_1(r\mu) d\mu,$$

and the corresponding streamfunction Ψ_0 induced by the presence of the tube:

$$\Psi_0 = \frac{\Gamma_0 R_0 r}{\pi} \int_0^\infty \frac{\mathrm{K}_1(\mu R_w)}{\mathrm{I}_1(\mu R_w)} \mathrm{I}_1(R_0\mu) \mathrm{I}_1(r\mu) \cos(x\mu) d\mu,$$

where K_1 is the modified Bessel function of the second kind.

is that the streamfuction Ψ_{VR} (from Model I) at large distances ($z = \theta\sqrt{x^2 + r^2} \to \infty$) tends to the streamfunction of a circular vortex filament Ψ:

$$\Psi_{VR} \approx \frac{\Gamma_0 R_0 r\theta}{4} \int_0^\infty [2\exp(-|x|\theta\mu)+\exp(-z^2/2)O(\frac{1}{z^2})]\mathrm{J}_1(r\theta\mu)\mathrm{J}_1(\theta\mu)d\mu$$

$$\approx \frac{\Gamma_0 R_0 r\theta}{2} \int_0^\infty \exp(-|x|\theta\mu)\mathrm{J}_1(\theta\mu)\mathrm{J}_1(r_1\theta\mu)d\mu$$

$$= \frac{\Gamma_0 R_0 r}{2} \int_0^\infty \exp(-|x|\mu)\mathrm{J}_1(R_0\mu)\mathrm{J}_1(r\mu)d\mu.$$

Resulting streamfuction:

$$\Psi_{VRC} = \frac{\Gamma_0 R_0 \sigma}{4} \int_0^\infty [\exp(\eta\mu)\mathrm{erfc}(\frac{\mu+\eta}{\sqrt{2}}) + \exp(-\eta\mu)\mathrm{erfc}(\frac{\mu-\eta}{\sqrt{2}})]$$

$$\times J_1(\theta\mu) J_1(\sigma\mu) d\mu - \frac{\Gamma_0 R_0 r}{\pi} \int_0^\infty \frac{K_1(\mu R_w)}{I_1(\mu R_w)} I_1(R_0\mu) I_1(r\mu) \cos(x\mu) d\mu$$

Vortex ring with a core of circular cross- section in a tube, Model III

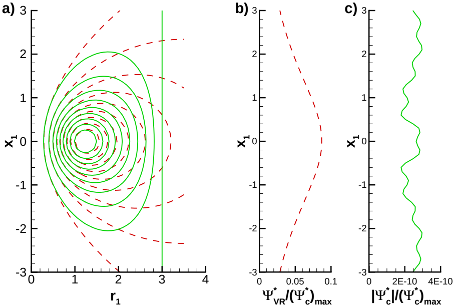

Figure: (a) Isocontours of the normalised streamfunctions $\Psi_c/(\Psi_c)_{max}$ for a confined ring for $\varepsilon = 1/3, \theta = 3$ (solid curves), and $\Psi_{VR}/(\Psi_{VR})_{max}$ for an unbounded ring with $\theta = 3$ (dashed curves). Contours are shown for $\Psi_c/(\Psi_c)_{max}$ from 0.1 to 0.9 with an increment of 0.1. The vertical line at $r_1 = 3$ represents the tube wall for the confined ring. Profiles along the tube wall line ($r_1 = 3$) for Ψ_{VR} (b) and $|\Psi_c|$ (c).

Comparison between the DNS and Model III (thanks to Ionut Danaila)

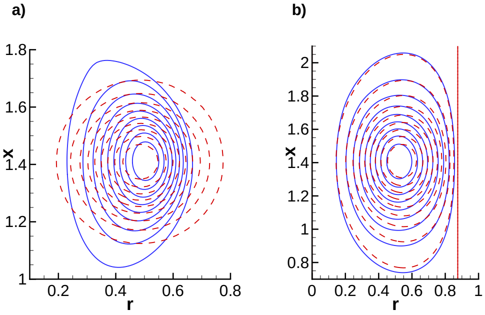

Figure: Comparison between the DNS data (blue solid curves) and predictions of the vortex ring model (red dashed curves). Contours of normalised vorticity ω/ω_{max} (a) and corresponding normalised streamfunction ψ/ψ_{max} (b). Values of ω/ω_{max} and ψ/ψ_{max} from 0.1 to 0.9 with increments of 0.1 are shown. $Re = 1700$, $D_w/D = 1.75$, $t = 8$.

Concluding Remarks

- In this case we have not ready-made formulae for the circulation, kinetic energy and translational velocity. All characteristics of vortex rings can be obtained by integrating of Ψ_{VRC} and ω_{VR}.
- For typical values $3 \leq \theta \leq 4.5$ most relevant to practical applications (Danaila& Helie 2008; Fukumoto 2010), the confined vortex ring model can be applied with negligible errors for all confinement parameters $\varepsilon \geq 0.875, \varepsilon = R_0/R_w < 1$,(Danaila et al., JFM 2015).

Vortex ring with a core of elliptic cross- section in a tube, Model IV

The streamfunction of the vortex ring with the elliptical shape of the core in regular coordinates:

$$\Psi_{VRE} = \frac{\Gamma_0 \theta r}{4R_0} \int_0^\infty \exp(\frac{\beta^2 - 1)\mu^2}{2} [\exp(\mu \frac{x\theta}{R_0}) \mathrm{erfc} \left(\frac{\mu\beta + x\theta/(R_0\beta)}{\sqrt{2}} \right)$$

$$+ \exp(-\mu \frac{x\theta}{R_0}) \mathrm{erfc} \left(\frac{\mu\beta - x\theta/(R_0\beta)}{\sqrt{2}} \right)] \mathrm{J}_1 (\theta\mu) \mathrm{J}_1 \left(\frac{r\theta}{R_0} \mu \right) d\mu,$$

which at the large distances for $z = \theta\sqrt{x^2 - r^2} \to \infty$ tends to

$$\Psi_{VRE} \approx \Gamma_0 \frac{r}{2} \int_0^\infty \exp((\beta^2 - 1) \frac{R_0^2}{2\theta^2} \mu^2) \exp(-|x|\mu) \mathrm{J}_1 (R_0\mu) \mathrm{J}_1 (r\mu) d\mu.$$

Finding of the streamfunction induced by the presence of the tube

- The idea behind the Brasseour's approach was to find such streamfunction (Green function to Laplace's equation with Neumann boundary condition and treated as induced by the presence of the tube) which being combined with the circular vortex filament (CVF) would satisfy the corresponding boundary condition of no flow on the wall.
- The streamfunction for the theoretical vortex ring with elliptical core is different from CVF that prevents direct using of the Brasseour's additional streamfunction.
- We use a power series of $\exp((\beta^2 - 1)R_0^2\mu^2/(2\theta^2)$ in ϵ_0:

$$\Psi_{VRE} \approx \Gamma_0 \frac{r}{2} \int_0^{\infty} (1 + \frac{R_0^2\mu^2\epsilon_0}{\theta^2} + \frac{R_0^2\mu^2(\theta^2 + R_0^2\mu^2)\epsilon_0^2}{2\theta^4} + ...)$$

$$\times \exp(-|x|\mu) \mathrm{J}_1(R_0\mu)\mathrm{J}_1(r\mu) d\mu.$$

and find the superposition of the solutions, that correspond to the all terms of the above expansion.

The potential function corresponding to the latter streamfunction:

$$\Phi_{VRE} = -\frac{\Gamma_0 R_0}{2} \int_0^\infty (1 + \frac{R_0^2 \mu^2 \epsilon_0}{\theta^2} + \frac{R_0^2 \mu^2 (\theta^2 + R_0^2 \mu^2) \epsilon_0^2}{2\theta^4} + ...)$$
$$\times \exp(-|x|\mu) \mathrm{J}_1(R_0 \mu) \mathrm{J}_0(r\mu) d\mu.$$

Using the parameter $0 < \varepsilon < 1$, which quantifies the confinement of the vortex ring, we can transform the potential function to the outer variables

$$\Phi_{VRE} = -\Gamma_0 \frac{\varepsilon}{2} \int_0^\infty (1 + \frac{R_0^2 \mu^2 \epsilon_0}{\theta^2} + \frac{R_0^2 \mu^2 (\theta^2 + R_0^2 \mu^2) \epsilon_0^2}{2\theta^4} + ...)$$
$$\times \exp(-|\tilde{x}|\mu) \mathrm{J}_1(\varepsilon \mu) \mathrm{J}_0(\tilde{r}\mu) d\mu,$$

where

$$\tilde{x} = \frac{x}{R_w}, \quad \tilde{r} = \frac{r}{R_w}, \quad \varepsilon = \frac{R_0}{R_w}.$$

Applying the expansion of $\mathrm{J}_1(\varepsilon\mu)$ of ε

$$\mathrm{J}_1(\varepsilon\mu) = \frac{\varepsilon\mu}{2} - \frac{(\varepsilon\mu)^3}{16} + \frac{(\varepsilon\mu)^5}{284} + ...,$$

and using that

$$\frac{\partial^n}{\partial x^n}\exp(-\mu x) = (-\mu)^n \exp(-\mu x),$$

we can represent the potential function in the following form

$$\Phi_{VRE} = \Gamma_0 \frac{\varepsilon}{2}\left(\frac{\varepsilon}{2}\frac{\partial}{\partial \tilde{x}} - \frac{\varepsilon^3}{16}\frac{\partial^3}{\partial \tilde{x}^3} + \frac{\varepsilon^5}{284}\frac{\partial^5}{\partial \tilde{x}^5} - \dots\right)$$

$$\times\left[\int_0^\infty \left(1 + \frac{R_0^2\mu^2\epsilon_0}{\theta^2} + \frac{R_0^2\mu^2(\theta^2 + R_0^2\mu^2)\epsilon_0^2}{2\theta^4} + \dots\right)\exp(-|\tilde{x}|\mu)J_0(\tilde{r}\mu)d\mu\right]$$

$$= \Gamma_0 \frac{\varepsilon}{2}\left(\frac{\varepsilon}{2}\frac{\partial S}{\partial \tilde{x}} - \frac{\varepsilon^3}{16}\frac{\partial^3 S}{\partial \tilde{x}^3} + \frac{\varepsilon^5}{284}\frac{\partial^5 S}{\partial \tilde{x}^5} - \dots\right)$$

It can be seen that the behavior of the potential function at the far distances is defined by the expression S, which for $\epsilon_0 = 0$ represents the point dipole. The basic idea behind the Brasseour method is to replace the form S by other form Q with the aim to satisfy the boundary condition on the tube wall

$$\frac{\partial Q}{\partial \tilde{r}} = 0 \quad at \quad \tilde{r} = 1$$

or, on the other words, to find Green function to Laplace's equation with the Neumann boundary condition that must satisfy:

$$\nabla^2 Q = 4\pi\delta(\vec{x}).$$

Keeping in mind the integrals

$$D_1 = \int_0^\infty \exp(-|\tilde{x}|\mu) \mathrm{J}_0(\tilde{r}\mu) d\mu = \frac{1}{\sqrt{(\tilde{x}^2 + \tilde{r}^2)}},$$

$$D_2 = \int_0^\infty \mu^2 \exp(-|\tilde{x}|\mu) \mathrm{J}_0(\tilde{r}\mu) d\mu = \frac{(-\tilde{r}^2 + 2\tilde{x}^2)}{(\tilde{x}^2 + \tilde{r}^2)^{5/2}},$$

$$D_3 = \int_0^\infty \mu^4 \exp(-|\tilde{x}|\mu) \mathrm{J}_0(\tilde{r}\mu) d\mu = \frac{3(3\tilde{r}^4 - 24\tilde{r}^2\tilde{x}^2 + 8\tilde{x}^4)}{(\tilde{x}^2 + \tilde{r}^2)^{9/2}},$$

we can to define

$$S = D_1 + \frac{R_0^2\epsilon_0}{\theta^2}D_2 + \frac{R_0^2\epsilon_0^2}{2\theta^4}(D_2 + R_0^2 D_3) + ...$$

and to search a sought function in the following form:

$$Q = [D_1 + \int_0^\infty f_1(\mu)\mathrm{I}_0(\tilde{r}\mu)\cos(\mu\tilde{x})d\mu]$$

$$+[(\frac{R_0^2\epsilon_0}{\theta^2} + \frac{R_0^2\epsilon_0^2}{2\theta^2})D_2 + \int_0^\infty f_2(\mu)\mu^2\mathrm{I}_0(\tilde{r}\mu)\cos(\mu\tilde{x})d\mu]$$

$$+[\frac{R_0^4\epsilon_0^2}{2\theta^4}D_3 + \int_0^\infty f_3(\mu)\mu^4\mathrm{I}_0(\tilde{r}\mu)\cos(\mu\tilde{x})d\mu] + ...$$

Using other representations of the integrals D_1, D_2 and D_3

$$D_1 = \frac{1}{\sqrt{(\tilde{x}^2 + \tilde{r}^2)}} = \frac{2}{\pi}\int_0^\infty \mathrm{K}_0(\tilde{r}\mu)\cos(\mu\tilde{x})d\mu,$$

$$D_2 = \frac{(-\tilde{r}^2 + 2\tilde{x}^2)}{(\tilde{x}^2 + \tilde{r}^2)^{5/2}} = -\frac{2}{\pi}\int_0^\infty \mu^2 \mathrm{K}_0(\tilde{r}\mu)\cos(\mu\tilde{x})d\mu,$$

$$D_3 = \frac{3(3\tilde{r}^4 - 24\tilde{r}^2\tilde{x}^2 + 8\tilde{x}^4)}{(\tilde{x}^2 + \tilde{r}^2)^{9/2}} = \frac{2}{\pi}\int_0^\infty \mu^4 \mathrm{K}_0(\tilde{r}\mu)\cos(\mu\tilde{x})d\mu,$$

we can to rewrite Q in the other form

$$Q = \int_0^\infty ([\frac{2}{\pi}\mathrm{K}_0(\tilde{r}\mu) + f_1(\mu)\mathrm{I}_0(\tilde{r}\mu)]\cos(\mu\tilde{x})$$

$$+[(\frac{R_0^2\epsilon_0}{\theta^2} + \frac{R_0^2\epsilon_0^2}{2\theta^2})(-\frac{2}{\pi})\mathrm{K}_0(\tilde{r}\mu) + f_2(\mu)\mathrm{I}_0(\tilde{r}\mu)]\mu^2\cos(\mu\tilde{x})$$

$$+[\frac{R_0^4\epsilon_0^2}{2\theta^4}(\frac{2}{\pi})\mathrm{K}_0(\tilde{r}\mu) + f_3(\mu)\mathrm{I}_0(\tilde{r}\mu)]\mu^4\cos(\mu\tilde{x}) + ...)d\mu.$$

The boundary condition requires that

$$f_1(\mu) = \frac{2}{\pi}\frac{\mathrm{K}_1(\tilde{r})}{\mathrm{I}_1(\tilde{r})},$$

$$f_2(\mu) = (\frac{R_0^2\epsilon_0}{\theta^2} + \frac{R_0^2\epsilon_0^2}{2\theta^2})(-\frac{2}{\pi})\frac{\mathrm{K}_1(\tilde{r})}{\mathrm{I}_1(\tilde{r})},$$

$$f_3(\mu) = \frac{R_0^4\epsilon_0^2}{2\theta^4}\frac{2}{\pi}\frac{\mathrm{K}_1(\tilde{r})}{\mathrm{I}_1(\tilde{r})}.$$

This allows to represent a total potential $Q = Q_0 + Q_1$ in the following form

$$Q = D_1 + (\frac{R_0^2\epsilon_0}{\theta^2} + \frac{R_0^2\epsilon_0^2}{2\theta^2})D_2 + \frac{R_0^4\epsilon_0^2}{2\theta^4}D_3$$

$$+\frac{2}{\pi}\int_0^\infty((1 - (\frac{R_0^2\epsilon_0}{\theta^2} + \frac{R_0^2\epsilon_0^2}{2\theta^2})\mu^2 + \frac{R_0^4\epsilon_0^2}{2\theta^4}\mu^4 + \ldots)\frac{\mathrm{K}_1(\tilde{r})}{\mathrm{I}_1(\tilde{r})}\mathrm{I}_0(\tilde{r}\mu)\cos(\mu\tilde{x}))d\mu.$$

Substituting Q_1 into latter expression, we receive

$$\Phi^0_{VREC} = \frac{\varepsilon\Gamma_0}{2}\left(\frac{\varepsilon}{2}\frac{\partial}{\partial\tilde{x}} - \frac{\varepsilon^3}{16}\frac{\partial^3}{\partial\tilde{x}^3} + \frac{\varepsilon^5}{284}\frac{\partial^5}{\partial\tilde{x}^5} - \ldots\right)$$

$$\times\frac{2}{\pi}\int_0^\infty((1-(\frac{R_0^2\epsilon_0}{\theta^2}+\frac{R_0^2\epsilon_0^2}{2\theta^2})\mu^2+\frac{R_0^4\epsilon_0^2}{2\theta^4}\mu^4+...)$$

$$\times\frac{\mathrm{K}_1(\tilde{r})}{\mathrm{I}_1(\tilde{r})}\mathrm{I}_0(\tilde{r}\mu)\cos(\mu\tilde{x}))d\mu.$$

Performing the differentiation by $\tilde{x}$

$$\Phi^0_{VREC}=-\frac{\varepsilon\Gamma_0}{\pi}\int_0^\infty[\frac{\varepsilon\mu}{2}+\frac{\varepsilon^3\mu^3}{16}+\frac{\varepsilon^5\mu^5}{284}+...])$$

$$\times((1-(\frac{R_0^2\epsilon_0}{\theta^2}+\frac{R_0^2\epsilon_0^2}{2\theta^2})\mu^2+\frac{R_0^4\epsilon_0^2}{2\theta^4}\mu^4+...)\frac{\mathrm{K}_1(\tilde{r})}{\mathrm{I}_1(\tilde{r})}\mathrm{I}_0(\tilde{r}\mu)\sin(\mu\tilde{x}))d\mu$$

and recognizing the expression in the square brackets as $\mathrm{I}_1(\varepsilon\mu)$, we we can define the potential field induced by the presence of the tube on a vortex ring with elliptical core as

$$\Phi^0_{VREC}=-\frac{\Gamma_0\varepsilon}{\pi}\int_0^\infty(1-(\frac{R_0^2\epsilon_0}{\theta^2}+\frac{R_0^2\epsilon_0^2}{2\theta^2})\mu^2+\frac{R_0^4\epsilon_0^2}{2\theta^4}\mu^4+...)$$

$$\times \frac{\mathrm{K}_1(\tilde{r})}{\mathrm{I}_1(\tilde{r})} \mathrm{I}_0(\tilde{r}\mu)\mathrm{I}_1(\varepsilon\mu)\sin(\mu\tilde{x}))d\mu.$$

This result in the regular variables becomes

$$\Phi^0_{VREC} = -\frac{\Gamma_0 R_0}{\pi} \int_0^\infty (1 - (\frac{R_0^2 \epsilon_0}{\theta^2} + \frac{R_0^2 \epsilon_0^2}{2\theta^2})\mu^2 + \frac{R_0^4 \epsilon_0^2}{2\theta^4}\mu^4 + ...)$$

$$\times \frac{\mathrm{K}_1(rR_w)}{\mathrm{I}_1(rR_w)} \mathrm{I}_0(r\mu)\mathrm{I}_1(\mu R_0)\sin(\mu x))d\mu.$$

From the relations

$$\frac{1}{r}\frac{\partial \Psi}{\partial x} = \frac{\partial \Phi}{\partial r} \quad -\frac{1}{r}\frac{\partial \Psi}{\partial r} = \frac{\partial \Phi}{\partial x}$$

we can also find the streamfunction induced by the presence of the tube

$$\Psi^0_{VREC} = \frac{\Gamma_0 R_0}{\pi} r \int_0^\infty (1 - \frac{R_0^2}{\theta^2}\mu^2 \epsilon_0 + (-\frac{R_0^2}{2\theta^2}\mu^2 + \frac{R_0^4}{2\theta^4}\mu^4)\epsilon_0^2 + ...)$$

$$\times \frac{\mathrm{K}_1(rR_w)}{\mathrm{I}_1(rR_w)} \mathrm{I}_1(r\mu)\mathrm{I}_1(\mu R_0)\cos(\mu x))d\mu$$

and represent it in the dimensionless form

$$\Psi^{0*}_{VREC} = \frac{r_1}{\pi}\int_0^{\infty}(1 - \frac{1}{\theta^2}\mu^2\epsilon_0 + (-\frac{1}{2\theta^2}\mu^2 + \frac{1}{2\theta^4}\mu^4)\epsilon_0^2 + ...)$$

$$\times \frac{\mathrm{K}_1(\mu/\epsilon)}{\mathrm{I}_1(\mu/\epsilon)} \mathrm{I}_1(r_1\mu)\mathrm{I}_1(\mu)\cos(\mu x_1))d\mu.$$

Rewriting the basic streamfunction Ψ^*_{VRE} also in the dimensionless form

$$\Psi^*_{VRE} = \frac{\theta^2 r_1}{4} \int_0^\infty \exp(\frac{\beta^2 - 1)\mu^2}{2} [\exp(\mu x_1 \theta) \mathrm{erfc} \left(\frac{\mu\beta + x_1(\theta/\beta)}{\sqrt{2}} \right)$$

$$+ \exp(-\mu x_1 \theta) \mathrm{erfc} \left(\frac{\mu\beta - x_1(\theta/\beta)}{\sqrt{2}} \right)] \mathrm{J}_1\left(\theta\mu\right) \mathrm{J}_1\left(r_1\theta\mu\right) d\mu,$$

we find the sought streamfunction corresponding to a confined elliptical vortex ring as

$$\Psi^*_{VREC} = \Psi^*_{VRE} - \Psi^{0*}_{VREC}$$

This streamfunction is identical with the Brasseour's result for $\epsilon_0 = 0$. To illustrate the difference of the streamlines for confined vortex rings with the elliptical ring's cores, we plot the contours predicted by the streamfunction Ψ^*_{VREC} for different values of ϵ_0 in the following figure:

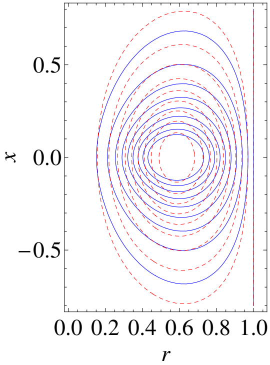

Figure: Isocontours of the normalised streamfunctions ($\Psi^*_{VREC}/\Psi^*_{VREC\,max}$) for a confined vortex ring with elliptical core predicted by Model IV for two values of ε_0: $\varepsilon_0 = 0.5$ (red dashed curves); $\varepsilon_0 = -0.5$ (blue solid curves). Other parameters were taken as $\epsilon = 0.5$; $R_0 = 0.535$; $L = 0.13$; $\Gamma_0 = 0.714$; $\theta = R_0/L = 4.099$ for both cases. Contours are shown for ($\Psi^*_{VREC}/\Psi^*_{VREC\,max}$) from 0.1 to 0.9 with an increment of 0.1.

The obtained streamfunction Ψ^*_{VREC} with the vorticity ω^*_{VR} (Model I) may serve as an approximation of the solution of the problem of viscous vortex ring in a tube.

Finding of ϵ_0 ($\beta = 1 + \epsilon_0$) and λ_0 ($\lambda = 1 + \lambda_0$) for $Re = 1700$ and $D_w/D = 3$

$$\tilde{E}_\mathrm{n} = E/(M^{1/2}\Gamma^{3/2}),$$
$$\tilde{\Gamma}_\mathrm{n} = \Gamma/(M^{1/3}U^{2/3}).$$

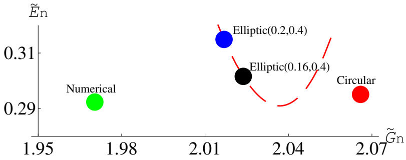

Figure: Comparison between DNS data (by I. Danaila) and model prediction for the normalized energy and circulation

Comparison between DNS data (by I. Danaila) and model prediction for kinetic energy for different confinement parameters and $Re = 1700$

a) b)

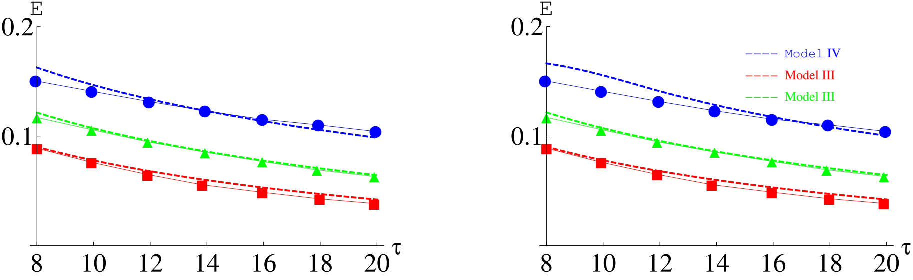

Figure: Time evolution of the kinetic energy E of the vortex ring for $Re = 1700$. a)Comparison between the DNS data and prediction of the Model III, Danaila et al., JFM 2015, Fig. 10). b)Comparison between the DNS data and prediction of different models.

Comparison between DNS data (by I. Danaila) and model prediction for translational velocity for different confinement parameters and $Re = 1700$

a) 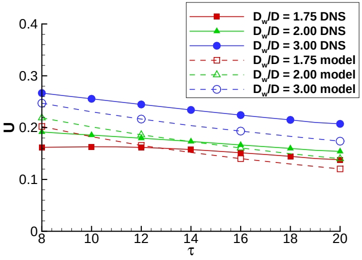

b) 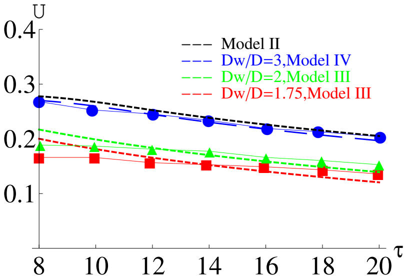

Figure: Time evolution of the translational velocity U of the vortex ring for $Re = 1700$. a)Comparison between the DNS data and prediction of the Model III, Danaila et al., JFM 2015, Fig. 17). b)Comparison between the DNS data and prediction of different models.

Comparison between DNS data (by I. Danaila) and model prediction for kinetic energy for different confinement parameters and $Re = 3400$

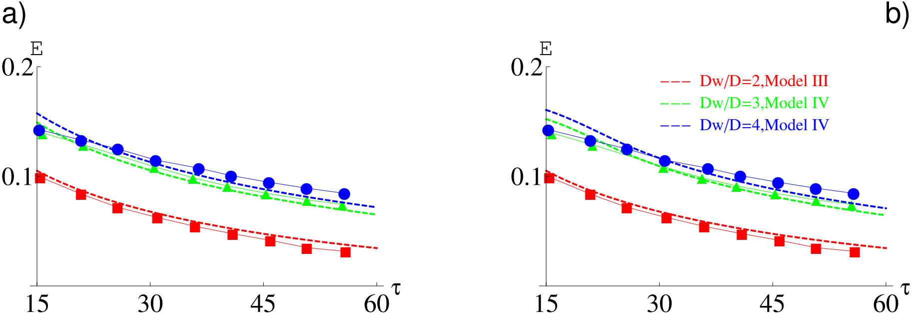

Figure: Time evolution of the kinetic energy E of the vortex ring for $Re = 3400$. a)Comparison between the DNS data and prediction of the Model III, Danaila et al., JFM 2015, Fig. 10). b)Comparison between the DNS data and prediction of different models.

Comparison between DNS data (by I. Danaila) and model prediction for translational velocity for different confinement parameters and $Re = 3400$

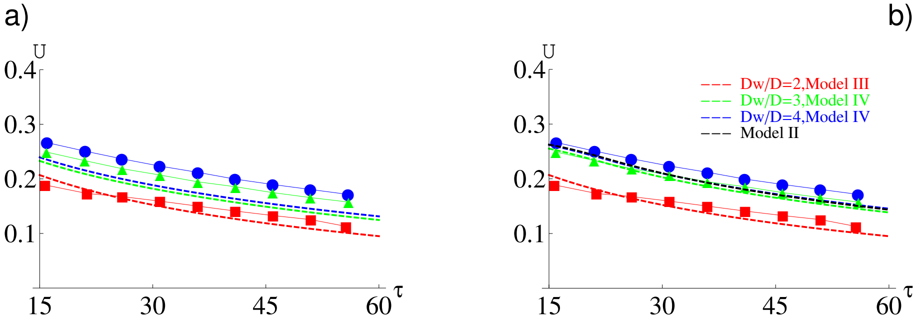

Figure: Time evolution of the translational velocity U of the vortex ring for $Re = 3400$. a)Comparison between the DNS data and prediction of the Model III, Danaila et al., JFM 2015, Fig. 17). b)Comparison between the DNS data and prediction of different models.

a)

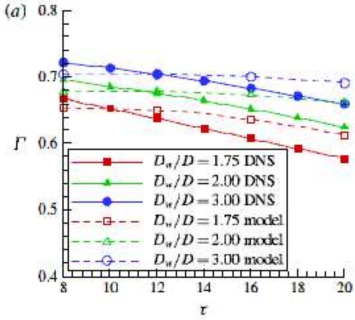

b)

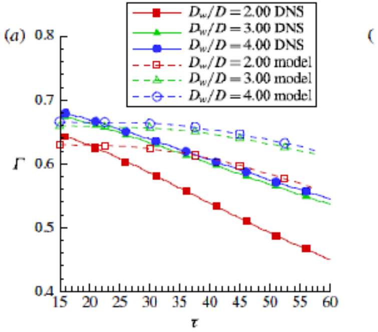

Figure: Time evolution of the circulation Γ of the vortex ring for $Re = 1700$ (a) and $Re = 3400$ (b).

Concluding remarks

The circulation of the confined vortex rings very rapidly reduces with time that leads to low-Reynolds number flow regime and allows to successfully apply Model III. When the effect of the confinement is small ($Dw/D > 3$) we can use Model II. If not one of these effects is not dominated the Model IV is preferable.

Prediction of the formation number (kinematic approach, Shusser&Gharib, PF 2000)

Criterium for the pinch-off:

$$U = \frac{D^2}{4R_0^2} U_p$$

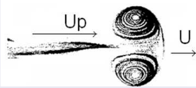

By introducing

$$B(\theta) = U(\theta)\sqrt{\frac{\pi M}{\Gamma(\theta)^3}},\ b_s(\theta) = R_0\sqrt{\frac{\pi\Gamma(\theta)}{2M}},\ M = \pi\Gamma_0 R_0^2$$

we receive from the slug - flow approximation

$$\frac{L}{D} = \frac{\sqrt{2}\pi}{4b_s(\theta)^2 B(\theta)} \text{ and } \alpha(\theta) = \frac{E(\theta)}{\sqrt{M\Gamma(\theta)^3}},\ \alpha(\theta) \geq \frac{2B(\theta)b_s(\theta)^2}{\sqrt{\pi}}$$

Results and plans

- The model for the unconfined vortex ring (Model I) predicts the formation number $L/D = 3.5$ for $\nu t/R_0^2 \approx 0.0213$ ($\theta \approx 4.85$) on the basis of the criteria by Shusser&Gharib (PF, 2000).
- The model for confined vortex ring ($D_w/D = 1.75$) with a core of circular cross- section (Model III) predicts the formation number $L/D = 1.8$ at $\tau \approx 2.22$ ($\theta \approx 7.2$) and the model for confined vortex ring with a core of elliptical cross- section (Model IV) predicts $L/D = 1.5$ at $\tau \approx 1.31$ ($\theta \approx 11.25$) based on the same criteria.
- The DNS (Danaila et al, JFM 2015) for the confined vortex ring ($D_w/D = 1.75, \tau = 2.26$) allows to obtain the stroke length: $L_p = 1.28$. It is lower than the so-called formation number (3.5 - 4.5) and corresponds to the case when the vorticity produced by the vortex generator is not completely engulfed by the vortex ring (differently from the case of the "optimal" vortex ring formation).
- In the future we plan to develop the predicting of the stroke length for confined vortex ring.